PHYSICAL REVIEW E **76**, 055402(R) (2007)

Bubble regime for ion acceleration in a laser-driven plasma

Baifei Shen,[1,2,3] Yuelin Li,[2,3] M. Y. Yu,[4] and John Cary[5,6]
[1]*Shanghai Institute of Optics and Fine Mechanics, P.O. Box 800-211, Shanghai 201800, China*
[2]*Accelerator Systems Division, Argonne National Laboratory, Argonne, Illinois 60439, USA*
[3]*Argonne Accelerator Institute, Argonne National Laboratory, Argonne, Illinois 60439, USA*
[4]*Institut für Theoretische Physik I, Ruhr-Universität Bochum, D-44780 Bochum, Germany*
[5]*Tech-X Corporation, Boulder, Colorado 80303, USA*
[6]*Department of Physics, University of Colorado, Boulder, Colorado 80309, USA*
(Received 12 February 2007; revised manuscript received 24 September 2007; published 9 November 2007)

Proton trapping and acceleration by an electron bubble-channel structure in laser interaction with high-density plasma is investigated by using three-dimensional particle-in-cell simulations. It is shown that protons can be trapped, bunched, and efficiently accelerated for appropriate laser and plasma parameters, and the proton acceleration is enhanced if the plasma consists mainly of heavier ions such as tritium. The observed results are analyzed and discussed in terms of a one-dimensional analytical three-component-plasma wake model.

DOI: 10.1103/PhysRevE.76.055402 PACS number(s): 52.38.Kd, 52.38.Hb, 52.65.Rr

Electron and ion acceleration in laser-driven plasmas has drawn wide attention due to its potential in realizing small-size ultrahigh-energy particle accelerators [1–8]. For ion acceleration, proton beams with maximum energy up to about 60 MeV have been observed [9,10] during irradiation of solid targets by terawatt and petawatt lasers. Successful production of quasimonoenergetic proton and carbon-ion bunches of several MeV/nucleon at the back surface of a microstructured thin solid target has been reported [7,8]. The protons and heavier ions are accelerated by the "target normal sheath acceleration" (TNSA) mechanism: the electrons in the front part of the thin-foil target are accelerated to ultrafast velocities by an intense short laser pulse, propagate through the target, and exit on the back side. An intense quasistatic electric field of the order of 10^{12} V/m is thus built up behind the rear target surface. The protons and other ions on the back foil surface are thus accelerated by this field until they neutralize the effect of the electrons. By microstructuring the rear foil surface or by focusing the charge-separation field, one can obtain monoenergetic ion bunches [7,8,11]. On the other hand, target ions can also be accelerated together with the electrons by high light pressures [12,13]. Three-dimensional simulation shows that several-GeV protons (maximum energy is about 3.2 GeV) can be obtained using an $a=eA/m_ec=316$ laser pulse with sharp pulse front [12]. Apart from these two mechanisms, ions can also be accelerated in the electrostatic shock front driven by an intense laser pulse [14–16]. In this case the electrons are first pushed, or snowplowed, outward by the laser ponderomotive force to form a dense electron layer (shock) in the front and on the side of the light pulse. If all the ions are reflected from the shock, then for a circularly polarized laser pulse the relativistic factor $\gamma_p=(1-v_p^2)^{-1/2}$ corresponding to the shock velocity v_p (normalized by the light speed c) can be calculated through momentum conservation and can be written as

$$\gamma_p = a/\sqrt{2nm_i} \tag{1}$$

in the ultrarelativistic limit while the ion velocity $v_i=2v_p/(1+v_p^2)$. In the nonrelativistic limit, the ion velocity is $2v_p$ and

$$v_p = a/\sqrt{nm_i}. \tag{2}$$

Here, m_i is the ion mass (normalized by the electron mass m_e) and n is the plasma density normalized by the critical density $n_c=m_e\omega_L^2/(4\pi e^2)$. Thus, high ion energy can be realized at low plasma density. Furthermore, at lower densities, more ions can go through the shock instead of being reflected, further reducing the number of accelerated ions, thus increasing their energy gain. On the other hand, we note that since the heavy ions respond slowly to the charge-separation field, an ultraintense electrostatic field is built up due to the high-density electron layer. The ions going through the dense electron layer and having proper speed can be trapped by this huge propagating electric field. The trapped ions, moving with and surfing on the field, can thus be accelerated over a long distance and achieve very large energy gain. This is similar to the scenario of particles being trapped and accelerated in a plasma wake.

Under proper conditions, a very efficient "bubble" regime can be realized. Recent investigation of the bubble regime [1–6] has demonstrated the generation of high-quality electron bunches with high energies up to 1 GeV, relatively small energy spread, and emittance approaching that of a conventional accelerator. While electrons are mainly accelerated at the rear of a bubble, ions can also be accelerated in the front of the bubble. At high plasma density and laser intensity, ions play an important role in forming the bubble structure as well as in electron and ion acceleration [17,18]. But only when ions are trapped in the wake field can they be accelerated efficiently. In this Rapid Communication we shall show that this is possible if both the plasma density and laser intensity are sufficiently high.

We shall first illustrate the proposed scheme using the three-dimensional particle-in-cell (PIC) simulation code VORPAL [19]. A circularly polarized laser pulse of wavelength 0.8 μm, normalized peak amplitude $a=316/\sqrt{2}$ [12,20], length 10 μm, and full width at half maximum (FWHM) spot size 16 μm enters from the left of the simulation box of size 400 μm$\times$80 μm$\times$80 μm. In this laser field, the vector potential normalized for protons is 0.17,

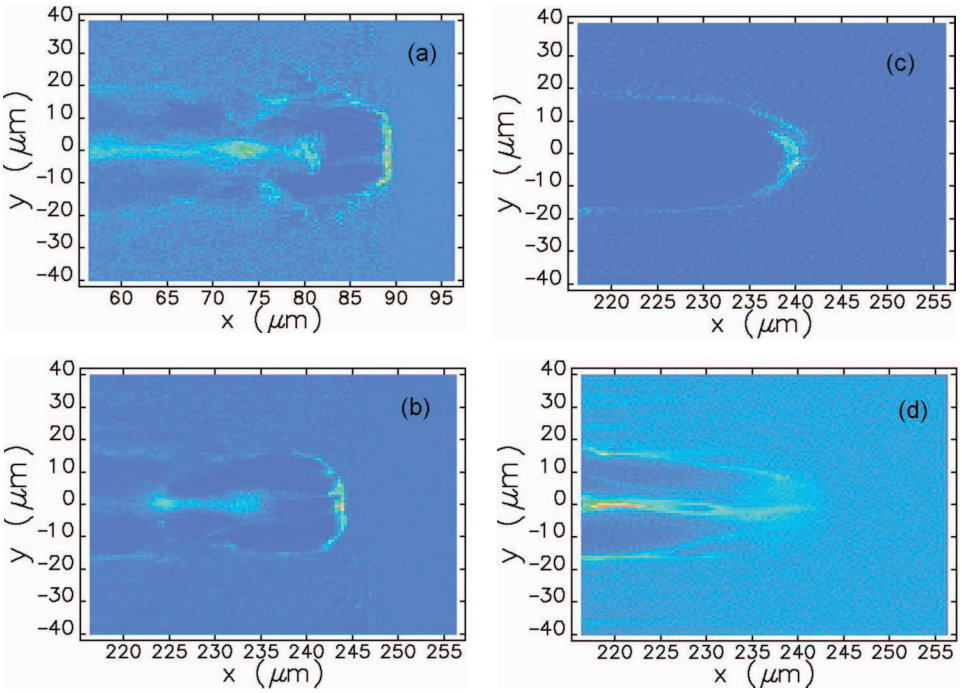

FIG. 1. (Color) Electron and ion density contour plots from the three-dimensional particle-in-cell simulation for a plasma with hydrogen density 1×10^{20} cm^{-3} and tritium density 1.4×10^{21} cm^{-3}. The laser pulse of wavelength 0.8 μm, normalized peak amplitude $a=316/\sqrt{2}$, length 10 μm, and FWHM spot size 16 μm enters from the left of the simulation box in the x direction. (a) Electron density at 320 fs; (b)–(d) electron, proton, and tritium ion density at 854 fs.

which is still smaller than 1. A plasma of electron density 1.5×10^{21} cm^{-3} and sharp boundaries is located in $8<x$ [μm]<400. So the density is slightly smaller than the critical density n_c. There are $1200\times100\times100$ cells in the simulation windows. The particle number per simulation cell for electron, proton, and tritium is 2 for a density of 1.5×10^{21} cm^{-3}. Open boundaries are used longitudinally and periodic boundaries are used transversally. With this condition, if a shock is formed and all the ions in front of the shock are reflected, from the estimate, Eq. (1), we obtain $\gamma_p=3.96$ for a pure hydrogen plasma and $\gamma_p=2.28$ for a pure tritium plasma. However, in reality this is not the case since the ion motion will significantly decrease the scalar potential, and thus ions cannot be trapped. On the other hand, if the plasma consists of mainly heavy ions, the light ions, or protons, can be easily trapped and accelerated. Therefore, in the simulation we consider a plasma with hydrogen density 1×10^{20} cm^{-3} and tritium density 1.4×10^{21} cm^{-3}.

Figure 1 shows snapshots of the electron, proton, and tritium densities. We see in Fig. 1(a), for n_e at $t=320$ fs, that an electron bubble is formed but it is less wholesome as that under conditions optimum for electron acceleration [17]. In fact, the structure here is a combination of a bubble and a channel, with a low-density tail extending all the way to the plasma edge. Nevertheless, one can see that many electrons are trapped in the center of the front bubblelike region. The trapped electrons are accelerated to energies of several GeV. The energetic-electron density distribution is not smooth and shall be discussed elsewhere. At $t=854$ fs, the electron bubble continues to propagate and the entire structure becomes more channel-like, as can be seen in Fig. 1(b). When most of the laser pulse is absorbed and reflected, the wake will disappear. At the same time, one can see in Fig. 1(c) a well-defined proton channel with a high-density front consisting of many wake-field-trapped and -accelerated protons. The latter can reach energies in the tens of GeV range, as shown in Fig. 2(a). In Fig. 1(d) one can see that the tritium-ion density also contains a channel structure. Because of the high concentration and mass, the tritium ions play an important role in the formation and evolution of the plasma structure as the background. They are accelerated but not trapped in the wake field. A high-density region can be observed at the center of the channel, as discussed by Esirkepov *et al.* [21].

The momentum and energy spectrum of protons are shown in Fig. 2. We see that many protons are trapped in the wake field. In fact, in the cross section -10 μm$<(y,z)$

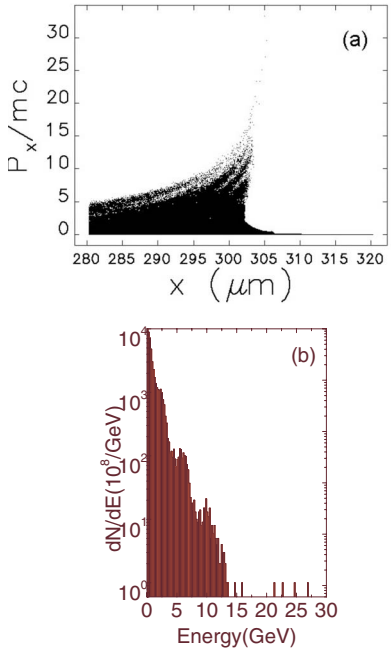

FIG. 2. (Color online) Momentum and energy spectrum of protons from the simlation in Fig. 1 at 1.067 ps.

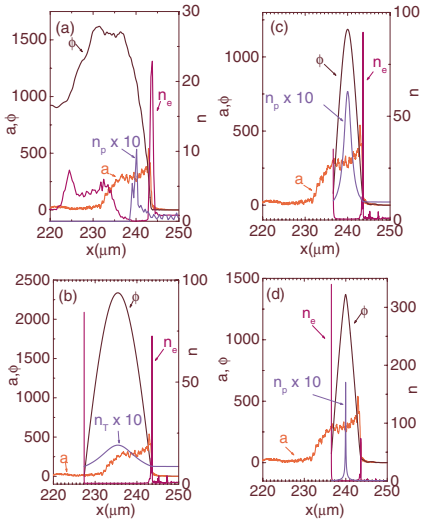

FIG. 3. (Color online) Simulation results at 854 fs (a) and analytical results for laser amplitude, scalar potential, electron density, and ion density in the case of pure tritium (b), pure proton (c), and 25% proton and 75% tritium (d). For the analytical results (b)–(d), the laser amplitude and the bubble speed are obtained from the simulation.

<10 μm one finds 1.4×10^9 protons with energy larger than 5 GeV. The maximum proton energy is about 27 GeV. The simulation result demonstrates that at suitable laser and plasma parameters, protons in large numbers can indeed be trapped and accelerated by the electron bubble. Peaked energy spectra have been found in earlier simulations, but it is still unclear how to obtain well-peaked stable energy spectra [10]. Anyway, the successful demonstration of monoenergetic electron bunches in the bubble regime gives us more hope. Compared to the scheme using light pressure [12], here one can obtain much larger proton energy at the same laser intensity of $a=316$ and no sharp pulse front is needed for the present acceleration scheme.

In Fig. 3(a) the profiles of the vector potential of the laser and scalar potentials of the wake obtained from the PIC simulation are shown. The peak amplitude of the laser light is about $a=540$, which is larger than the initial amplitude because of self-focusing and reflection of laser light from the highly compressed electron layer. We recall that in a traditional electron bubble no such light reflection occurs at the bubble wall since the plasma density is much lower than the critical density for a relativistic laser pulse, n_c/a. The maximum normalized scalar potential is about $\phi=1600$, which is large enough to trap protons but not enough to trap tritium ions (see below). This is why, in the simulation, one finds that only the protons are accelerated. It is also of interest to note that here the scalar potential does not become negative. This is because at that time a large number of electrons have already been trapped in the bubble, thus altering the potential. The longitudinal as well as radial complexity of the electron bubble-channel structure also indicates that three-dimensional effects are important for the particle dynamics and field evolution.

We now present a one-dimensional analytical model, which describes fairly well the proton acceleration process in the bubble regime. The model is based on the wake-field equations and we shall follow the existing theory [17,22], but for a plasma containing two species of ions. Accordingly, the equations for the scalar potential and particle densities are

$$\frac{d^2\phi}{d\xi^2}=\frac{v_g}{1-v_g^2}\left(\frac{n_e\Psi_e}{R_e}-\frac{n_{i1}\Psi_{i1}}{R_{i1}}-\frac{n_{i2}\Psi_{i2}}{R_{i2}}\right), \tag{3}$$

$$n'_\alpha=n_\alpha v_g(\Psi_\alpha/R_\alpha-v_g)/(1-v_g^2), \tag{4}$$

where $\alpha=e$, $i1$, and $i2$ denote the electrons, protons, and tritium ions, respectively, $\Psi_\alpha=1+\rho_\alpha\phi$, $R_\alpha=[\Psi_\alpha^2-(1-v_g^2)(1+\rho_\alpha^2a^2)]^{1/2}$, $\rho_e=1$, $\rho_{i1}=-1/1836$, $\rho_{i2}=-1/5508$, and n_α represent the initial densities.

The motion of a proton is given by

$$\sqrt{1+p_x^2+\rho_{i1}^2a^2}-\rho_{i1}\phi-v_pp_x=h_0, \tag{5}$$

where p_x is longitudinal momentum and h_0 is an integration constant corresponding to the initial proton condition in front of the electron bubble. For protons initially at rest we have $h_0=1$. From the above equation we obtain

$$p_x=\frac{v_p(h_0+\rho_{i1}\phi)\pm\sqrt{(h_0+\rho_{i1}\phi)^2-(1-v_p^2)(1+\rho_{i1}^2a^2)}}{1-v_p^2}. \tag{6}$$

A proton is trapped if the peak scalar potential is high enough so that it can be accelerated to a velocity equal to the bubble velocity. Since $\rho_{i1}^2a^2\ll1$, we have $h_0+\rho_{i1}\phi=1/\gamma_p$.

Equations (3) and (4) are used to calculate the ion density profiles and wake scalar potentials. For the laser field and bubble speed we shall use the simulation results. Note that self-consistant soliton solutions [22,23] are not applicable here since the structure evolves constantly and no soliton is formed. By measuring the position of the peak electron density in front of the laser pulse at the times $t=320.135$ fs and $t=853.696$ fs, we find that the average velocity of the bubble in this period is about $v_p=0.968c$, or $\gamma_p=3.98$, which is larger than that from the shock model with full proton reflection. This implies that here there is only partial trapping of the protons. Using the trapping condition, for a proton or tritium ion initially at rest, a scalar potential of $\phi=1374$ or 4124 is needed for them to be trapped. Furthermore, for a transparent plasma we would have $v_p=1-n/(2a)=0.998$, which is considerably larger than that from the simulation. This is because even if initially the plasma is underdense for a relativistic laser pulse, the expelled (by the intense light pressure) electrons can form an overdense layer at the edge, especially in the front, of the laser pulse, so that the light will be reflected there. Figure 3(b) is for a pure tritium plasma. The peak scalar potential is found to be much larger than that from the simulation due to the lag of ion response, but still smaller than the necessary threshold (4124) for trapping due to its large mass. We should mention that our numerical solution stops at the base of the electron bubble. This is because here the electron density is too high and its profile too sharp: wave breaking can easily occur. Figure 3(c) is for a pure proton plasma. Here the peak scalar potential is much lower than that for a pure tritium plasma due to the quicker

response of the ions that mitigate the electron field. It is also lower than that in our simulation. Thus, despite their small mass, as the peak potential is lower than the threshold (1374) for trapping, the protons are not trapped. Figure 3(d) is for a plasma with 25% proton and 75% tritium ions. The proton density is chosen to be higher than that in the simulation, so that we are considering a case near wave breaking. In this case, the added tritium ions increase the scalar potential in comparison with Fig. 3(c) and the added protons supply the lighter ions to be trapped. We see that here the peak scalar potential from our model is close to the threshold (1374) for trapping and from the PIC simulation. The proton density near the peak of the scalar potential is very high. That is, protons in a plasma containing mainly heavy ions can be very efficiently trapped and accelerated by the electron bubble. In Fig. 3(d) a higher proton density and sharper profile in comparison with Figs. 3(b) and 3(c) are found, which indicates it is near wave breaking. For ions to be trapped, their velocity must be equal to the phase velocity of the wake; hence, the local density at the turning point would be infinitely high, but then it is impossible to calculate numerically.

In conclusion, a regime where protons can be efficiently trapped and accelerated by the electric fields of a dense layer of trapped electrons in the electron bubble region of the wake field is found by three-dimensional PIC simulation. When the plasma density is higher, it becomes the regime for shock acceleration, and when the plasma density is lower, protons cannot be properly trapped so that their acceleration is not efficient, since the potential is not large enough. A one-dimensional three-component-plasma model based on the corresponding modified wake equations is introduced and used to clarify the proton trapping and acceleration process. Proton acceleration by this mechanism is very effective when the protons are the minority ion component. This effect can be attributed to the fact that the heavier ions, due to their slow motion, contribute to the formation of an electron bubble with higher and longer-lasting electric field, so that the proton acceleration time is prolonged. For the region near the peak electron density at the front of the laser pulse, the agreement between the results of the model and the simulation is fairly good. Better agreement is not expected since the complex laser-plasma interaction process is clearly three dimensional. From the simulation results, we found that the proton energy scales with the laser intensity roughly as $I^{1/2}$. It is also found (not shown) that if the laser pulse is more intense, the electron bubble-channel structure is more stable. Filamentation instability also appears in the simulation, but the overall wake structure is not affected. For lower laser intensity, a higher plasma density is needed to supply a wake field large enough to trap the protons. And the scheme will gradually become ion acceleration by shock wave [14–16]. If the proton plasma of uniform density is replaced with a microstructer, such as a nanowire, a monoenergetic proton beam may be obtained with lower laser intensity.

This work is supported by the U.S. Department of Energy, Office of Science, Office of Basic Energy Sciences, under Contract No. DE-AC02-06CH11357. B.S. is in addition supported by China's NSFC Project No. 10675155 and 973 program. The authors thank K. J. Kim, K. Harkay, R. Stevens, H. Shang, and K. Nemeth for support. Computational time at the National Energy Research Scientific Computing center at LBNL is gratefully acknowledged.

[1] A. Pukhov and J. Meyer-ter-Vehn, Appl. Phys. B: Lasers Opt. **74**, 355 (2002).
[2] S. P. D. Mangles, C. D. Murphy, Z. Najmudin *et al.*, Nature (London) **431**, 535 (2004).
[3] C. G. R. Geddes, Cs. Toth, J. van Tilborg *et al.*, Nature (London) **431**, 538 (2004).
[4] J. Faure, Y. Glinec, A. Pukhov *et al.*, Nature (London) **431**, 541 (2004).
[5] W. P. Leemans, B. Nagler, A. J. Gonsalves, Cs. Toth, K. Nakamura, C. G. R. Geddes, E. Esarey, C. B. Schroeder, and S. M. Hokker, Nat. Phys. **2**, 696 (2006).
[6] J. Faure, C. Rechatin, A. Norlin, A. Lifschitz, Y. Glinec, and V. Malka, Nature (London) **444**, 737 (2006).
[7] H. Schwoerer, S. Pfotenhauer1, O. Jaeckel, K.-U. Amthor, B. Liesfeld, W. Ziegler, R. Sauerbrey, K. W. D. Ledingham, and T. Esirkepov, Nature (London) **439**, 445 (2006).
[8] B. M. Hegelich, B. J. Albright, J. Cobble, K. Flippo, S. Letzring, M. Paffett, H. Ruhl, J. Schreiber, R. K. Schulze, and J. C. Fernandez, Nature (London) **439**, 441 (2006).
[9] R. A. Snavely, M. H. Key, S. P. Hatchett *et al.*, Phys. Rev. Lett. **85**, 2945 (2000).
[10] D. Habs, G. Pretzler, A. Pukhov *et al.*, Prog. Part. Nucl. Phys. **46**, 375 (2001).
[11] T. Toncian, M. Borghesi, J. Fuchs, E. d'Humieres, P. Antici, P. Audebert, E. Brambrink, C. A. Cecchetti, A. Pipahl, L. Romagnani, and O. Willi, Science **312**, 410 (2006).
[12] T. Esirkepov, M. Borghesi, S. V. Bulanov, G. Mourou, and T. Tajima, Phys. Rev. Lett. **92**, 175003 (2004).
[13] B. Shen and Z. Xu, Phys. Rev. E **64**, 056406 (2001).
[14] A. Macchi, F. Cattani, T. V. Liseykina, and F. Cornolti, Phys. Rev. Lett. **94**, 165003 (2005).
[15] L. O. Silva, M. Marti, J. R. Davies, R. A. Fonseca, C. Ren, F. S. Tsung, and W. B. Mori, Phys. Rev. Lett. **92**, 015002 (2004).
[16] O. Shrokhov and A. Pukhov, Laser Part. Beams **22**, 175 (2004).
[17] S. V. Bulanov, M. Yamagiwa, T. Zh. Esirkepov, D. V. Dylov, F. F. Kamenets, N. S. Knyazev, J. K. Koga, M. Kando, Y. Ueshima, K. Saito, and D. Wakabayashi, Plasma Phys. Rep. **32**, 263 (2006).
[18] F. Yan, Z. M. Sheng, Q. L. Dong, J. Zhang, and W. Yu, J. Opt. Soc. Am. B **23**, 1190 (2006).
[19] C. Nieter and J. R. Cary, J. Comput. Phys. **196**, 448 (2004).
[20] T. Tajima and G. Mourou, Phys. Rev. ST Accel. Beams **5**, 031301 (2002).
[21] T. Zh. Esirkepov, Y. Sentoku, K. Mima, K. Nishihara, F. Califano, F. Pegoraro, N. M. Naumova, S. V. Bulanov, Y. Ueshima, T. V. Liseikina, V. A. Vshivkov, and Y. Kato, JETP Lett. **70**, 82 (1999).
[22] D. Farina and S. V. Bulanov, Phys. Rev. Lett. **86**, 5289 (2001).
[23] Baifei Shen, M. Y. Yu, and Ruxin Li, Phys. Rev. E **70**, 036403 (2004).